Chinese Chemical Letters 37 (2026) 111048

Contents lists available at ScienceDirect

Chinese Chemical Letters

journal homepage: www.elsevier.com/locate/cclet

Sterpiperazines A and B, steroid-indole alkaloids with Tdp1 inhibitory and chemotherapy sensitizing activities from marine fungus *Aspergillus* sp. EGF 15-0-3

Xia Wei[a,b,c,1], Zheng-Wu Luo[a,1], Guo-Qiang Zhang[a], Yan-An Lin[a], Ze-Kun Zhang[a], Lin-Kun An[d], Xi-Xin He[a], Jun-Cheng Su[c,*], Cui-Xian Zhang[a,*]

[a] *School of Pharmaceutical Sciences, Guangzhou University of Chinese Medicine, Guangzhou 510006, China*
[b] *Guangxi Key Laboratory of Bioactive Molecules Research and Evaluation, School of Pharmaceutical Sciences, Guangxi Medical University, Nanning 530021, China*
[c] *Key Laboratory for Chemistry and Molecular Engineering of Medicinal Resources (Ministry of Education of China), Guangxi Key Laboratory of Chemistry and Molecular Engineering of Medicinal Resources, School of Chemistry and Pharmaceutical Sciences, Guangxi Normal University, Guilin 541004, China*
[d] *School of Pharmaceutical Sciences, Sun Yat-sen University, Guangzhou 510006, China*

ARTICLE INFO

Article history:
Received 27 December 2024
Revised 4 March 2025
Accepted 6 March 2025
Available online 7 March 2025

Keywords:
Environmental-induced metabolites
Steroid-based indole alkaloids
Tdp1 inhibition
Chemotherapy sensitizing activities
Aspergillus sp. EGF 15-0-3

ABSTRACT

Hyperactivation of DNA repairing pathway is highly associated with the chemosensitivity and chemoresistance of cancer cells. In this manuscript, guided by cascaded one strain many compounds-global natural products social molecular networking (OSMAC-GNPS) strategy, a pair of epimeric environmental-induced metabolites were isolated from *Aspergillus* sp. EGF 15-0-3. Structurally, sterpiperazines A (**1**) and B (**2**) represent the first steroid-based indole alkaloids with unprecedented backbones. Biologically, compound **1** could be identified as a novel tyrosyl-DNA phosphodiesterase 1 (Tdp1) inhibitor with a unique mechanism distinct from the reported modulators, and was able to significantly enhance the sensitivity of NCI-H460 cells to the clinic chemotherapeutic drug through inhibiting the DNA repairment and enhanced the DNA damage of cancer cells.

© 2025 Published by Elsevier B.V. on behalf of Chinese Chemical Society and Institute of Materia Medica, Chinese Academy of Medical Sciences.

Tumors are malignant cells characterized by pathologic proliferation and rapid DNA replication [1,2]. Thus, compounds that block DNA replication continue to serve as potential anti-cancer agents [3], as exemplified by the clinical used chemotherapeutic drugs camptothecin (CPT) and its structural analogues topotecan (TPT) and irinotecan [4,5]. Mechanically, these natural product derivatives are topoisomerase I (Top1) inhibitors, which trap Top1-DNA complex through inserting the DNA nick made by Top1 during the DNA replication, leading to DNA damage, and eventually induce cancer cell death [6–9].

However, in response to drug treatment, cancer cells initiate different defensive mechanism *via* activating DNA repairment signalings, which are considered as a main reason for cancer drug resistance [10–12]. From this aspect, it is not surprising that numerous endeavors have been stimulated from the chemical and biological communities for discovering novel chemical entities that target DNA repairment feedback, such as represented by olaparib [13], gemcitabine [14], and pembrolizumab [15].

Natural products are functional metabolites produced by living organism during life process to adapt the external environment [16,17]. From this aspect, it is not surprising that those environmental-induced metabolites may serve as special candidates for identifying novel bioactive molecules [18,19]. To validate this hypothesis, during our previous investigation, the biosynthetic potential of *Aspergillus* sp. EGF 15–0–3, a soft coral-derived fungus, was performed by integrated one strain many compounds-global natural products social molecular networking (OSMAC-GNPS) strategy, which led to the identification of four unprecedented environmental-induced metabolites solely from the rice medium with selective cytotoxicities against human cancer cells [20]. Meanwhile, some unknown environmental-induced products with molecular weights ranging from 700 Da to 800 Da and distinct tandem mass spectrometry (MS/MS) fragments were observed (Figs. S1 and S2 in Supporting information). Inspired by these encouraging findings, a 900 L scaled-up recultivation of the title fungus was performed, provided two unusual steroid-based indole alkaloids sterpiperazines A (**1**) and B (**2**) (Fig. 1). Interest-

* Corresponding authors.
E-mail addresses: su_juncheng@163.com (J.-C. Su), zhangcuixian@gzucm.edu.cn (C.-X. Zhang).
[1] These authors contributed equally to this work.

https://doi.org/10.1016/j.cclet.2025.111048
1001-8417/© 2025 Published by Elsevier B.V. on behalf of Chinese Chemical Society and Institute of Materia Medica, Chinese Academy of Medical Sciences.

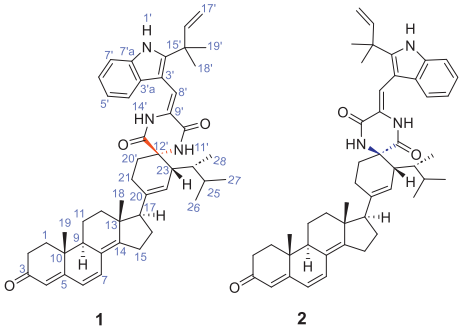


Fig. 1. Chemical structures of compounds **1** and **2**.

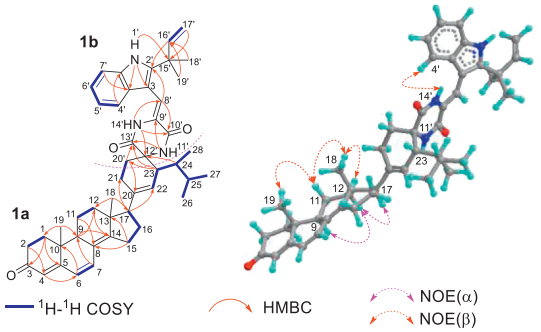


Fig. 2. ^{1}H–^{1}H COSY, key HMBC, and NOE correlations of **1**.

Table 1
^{1}H (600 MHz) and ^{13}C (150 MHz) NMR data of **1** in $CDCl_3$ (δ in ppm, J in Hz).[a]

No.	δ_H	δ_C	No.	δ_H	δ_C
1	a 1.36 (m)	35.3	23	3.07 (br s)	44.1
	b 1.89 (m)		24	1.52 (m)	39.0
2	a 1.84 (m)	34.3	25	1.63 (m)	33.6
	b 2.48 (m)		26	0.90 (d, 6.8)	20.7
3		199.6	27	0.89 (d, 6.8)	19.1
4	5.76 (s)	123.5	28	0.93 (d, 6.8)	13.1
5		164.2	1′	8.31 (s)	
6	6.08 (d, 9.2)	125.1	2′		143.7
7	6.60 (d, 9.2)	133.6	3′		103.0
8		125.4	3′a		126.3
9	2.17 (m)	44.7	4′	7.25 (d, 8.0)	118.9
10		36.9	5′	7.20 (t, 8.0)	122.4
11	a 1.59 (m)	19.3	6′	7.15 (t, 8.0)	121.1
	b 1.76 (m)		7′	7.36 (d, 8.0)	111.4
12	a 1.81 (m)	34.2	7′a		134.4
	b 1.99 (m)		8′	7.18 (s)	111.4
13		44.8	9′		124.9
14		154.0	10′		159.4
15	2.56 (m)	25.4	11′	6.09 (s)	
16	a 1.84 (m)	25.8	12′		62.1
	b 2.05 (m)		13′		168.2
17	2.15 (m)	56.3	14′	7.49 (s)	
18	0.90 (s)	20.3	15′		39.3
19	1.01 (s)	16.8	16′	6.07 (dd, 17.2, 10.6)	144.4
20		135.2	17′	5.22 (m)	113.6
21	a 2.16 (m)	25.2	18′	1.53 (s)	27.5
	b 2.34 (m)		19′	1.53 (s)	27.5
22	5.46 (s)	122.5	20′	2.31 (m)	34.4

[a] Overlapped signals are reported without designating multiplicity.

ingly, instead of showing direct growth inhibition to cancer cells, compound **1** significantly increased the sensitivity of NCI-H460 cells to chemotherapy drugs by tyrosyl-DNA phosphodiesterase 1 (Tdp1) inhibition *via* a unique binding mode, while its epimer **2** possessed weaker potency.

Sterpiperazine A (**1**) was obtained as white powder, with a molecular formula of $C_{47}H_{57}N_3O_3$ based on its high resolution electrospray ionization mass spectroscopy (HR-ESI-MS) *m/z* 712.4453 $[M+H]^+$ (calcd. for $C_{47}H_{58}N_3O_3$ 712.4478), corresponding to 21 degrees of unsaturation. The ultra violet (UV) spectrum displayed absorption maxima at 223, 270, and 347 nm. The IR spectrum suggested the presence of amine (3340, 3161, 3056 cm^{-1}), carbonyl (1756, 1685, 1629 cm^{-1}), as well as benzene ring (1560 and 1460 cm^{-1}) functionalities. The ^{1}H, ^{13}C nuclear magnetic resonance (NMR), and distortionless enhancement by polarization transfer (DEPT) spectra (Table 1) of **1** revealed the presence of one ketone carbonyl at δ_C 199.7, two amide carbonyls at δ_C 168.2 and 159.4, one tetrasubstituted double bonds at δ_C 154.0 and 125.4, three trisubstituted double bonds [δ_H 7.18 (1H, s), 5.76 (1H, s), and 5.51 (1H, s); δ_C 164.3, 135.1, 124.7, 123.4, 122.5, and 122.4], one *cis*-disubstituted double bond [δ_H 6.59 (1H, d, 9.2) and 6.07 (1H, d, 9.2); δ_C 133.7 and 125.0], one terminal double bond [δ_H 6.05 (1H, dd, 17.2, 10.8) and 5.20 (2H, m); δ_C 144.4 and 113.4], a 2,3-disubstituted indole moiety [δ_H 8.52 (1H, s), 7.36 (1H, d, 8.0), 7.23 (1H, d, 8.0), 7.18 (1H, t, 8.0), and 7.13 (1H, t, 8.0); δ_C 143.8, 134.5, 126.3, 121.0, 118.8, 111.5, 111.5, and 103.0], four quaternary carbons, five methines, eight methylenes, and seven methyls. Comprehensive analysis of 1D and 2D NMR data resulted in the full assignment of all the proton signals to their respective carbons (Table 1).

Eight spin-coupling systems could be established by the interpretation of the ^{1}H–^{1}H homonuclear correlation spectroscopy (COSY) spectrum of **1** (Fig. 2). In the heteronuclear multiple-bond correlation (HMBC) spectrum, correlations from H-1 to C-3/C-5, from H-2 to C-4, from H-4 to C-6, from H-6 to C-10, from H-7 to C-9, from H-9 to C-12/C-14, from H-11 to C-8, from H-12 to C-14, from H-15 to C-8/C-13, from H-17 to C-21/C-22, from H_3–18 to C-12/C-17, as well as from H_3–19 to C-1/C-9, suggested that the existence of steroid unit (**1a**, Fig. 2). Further comprehensive analysis of the ^{1}H and ^{13}C NMR data of remaining signals in **1** suggested the presence of a indole diketopiperazine fragment (**1b**, Fig. 2) and was confirmed by the HMBC correlations from NH-1′ to C-3′/C-3′a/C-15′, from H-4′ to C-3′/C-7′a, from H-7′ to C-3′a, from H-8′ to C-2′/C-10′, from NH-11′ to C-9′/C-13′, from NH-14′ to C-10′/C-12′, from H-16′ to C-2′, as well as from H-18′/H-19′ to C-16′, and from H-17′ to C-15′ (**1b**, Fig. 2). Finally, the connectivity of **1a** and **1b** *via* the C-21–C20′ and C-23–C12′ were concluded from the HMBC correlations from H-23 to C-13′/C-20′, from H-24 to C-12′, as well as from H-20′ to C-20/C-13′. Therefore, the planar structure of **1** was established as the first example of a steroid-based indole alkaloid.

As shown in Fig. 2, nuclear Overhauser effect (NOE) correlations of H-11a and H_3–19/H_3–18, indicated that H_3–18 and H_3–19 were cofacial and situated in the β-orientation. NOE correlations of H_3–18 and H-12b, H-17 and H-12a, as well as H-9 and H-12a, suggested H-9 and H-17 were in the α-orientation. Meanwhile, the double bond at C-8 was *Z*-geometry could be deduced by the NOE correlations of H-4′ and NH-14′. However, the relative configurations of the remaining stereocenters could not be firmly determined from the NMR data because of the lack of enough convincing NOE correlations. Fortunately, after various attempts, crystals with high quality of **1** for X-ray diffraction experiments were obtained from an optimized ternary solvent system (chloroform/methanol/water 9:1:0.5), and the relative and absolute configuration of **1** was determined as 9*S*, 10*R*, 13*R*, 17*S*, 23*R*, 24*R*, 12′*S* by the X-ray crystallographic analysis (Fig. 3, Flack parameter 0.008(12), CCDC 2083261).

Sterpiperazine B (**2**) was isolated as light yellow powder with the identical molecular formula to **1** based on its high resolution electrospray ionization mass spectroscopy (HRESIMS) at *m/z* 712.4406 $[M+H]^+$ (calcd. for $C_{47}H_{58}N_3O_3$ 712.4478). Comprehensive analysis of the NMR spectra of **1** and **2** indicated that both compounds shared the same planar structure (Table S1 and Fig. S3 in Supporting information). The major spectroscopic differences

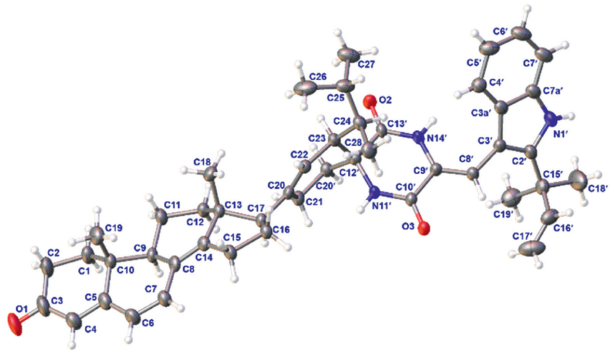


Fig. 3. X-ray Oak Ridge thermal ellipsoid plot (ORTEP) drawing of **1** at 30% ellipsoid probability.

between **1** and **2** could be attributed to C-12′ ($\Delta\delta$ −1.5), C-20′ ($\Delta\delta$ −4.9), as well as C-23 ($\Delta\delta$ +5.8), indicating that **2** was the 12′-epimer of **1** which was further supported by the observation of the NOE cross-peak of NH-11′ and H-23 (Fig. S3). The proposed structure of **2** was confirmed and its relative configurations were determined to be 9*S**, 10*R**, 13*R**, 17*S**, 23*R**, 24*R**, 12′*R** by using single-crystal X-ray diffraction analysis (Fig. S4 in Supporting information, Flack parameter 0.1(3), CCDC 2336492). The absolute configuration of **2** was further established as 9*S*, 10*R*, 13*R*, 17*S*, 23*R*, 24*R*, 12′*R* by using the quantum chemical electronic circular dichroism (ECD) calculation (Fig. S5 in Supporting information).

Tdp1 is an enzyme that plays crucial role in DNA repairment [21]. From the structural view, Tdp1 features three main binding pockets. Among which, the single-stranded DNA binding pocket and the Top1-derived peptide binding pocket synergistically work as the "trapper" to capture Top1-DNA cleavage complex (Top1cc), whereas the catalytic pocket is responsible for hydrolyzing the 3′-phosphotyrosyl bonds formed by topoisomerases during DNA replication [22]. Upregulation of Tdp1 is considered as a defensive feedback of tumor cells in response to chemotherapeutic drugs exposure and is the major causality of drug-resistance [21]. Although it was demonstrated that inhibition of Tdp1 improved the sensitivity of tumor cells to chemotherapeutic drugs, to date, no inhibitor was undergoing preclinical or clinical studies [23].

Structurally, compounds **1** and **2** are the first steroid-based indole alkaloids featuring a novel skeleton, which had never been reported before. However, a previous study of steroid derivatives indicated that, decoration of steroid with aromatic moiety at the northeastern side chain enhanced the Tdp1 inhibitory effects of these molecules [24]. Inspired by this finding, we wonder whether compounds **1** and **2**, which feature an aromatic indole diketopiperazine moiety at the side chain, possess the similar bioactivity. As a result, **1** showed significant Tdp1 inhibition in a dose-dependent manner with a half maximal inhibitory concentration (IC_{50}) value of 5.04 ± 0.48 μmol/L, while its C-12′ epimer **2** showed relative weak potency with an IC_{50} value of 17.23 ± 0.77 μmol/L.

In accordance with the biochemical results, molecular modeling of **1** showed clear interaction between the indole diketopiperazine moiety of **1** with the Top1-derived peptide binding pocket, whereas the steroid moiety deeply anchored in the catalytic pocket *via* forming two hydrogen bonds with Lys495 (2.2 Å) and Asn516 (1.7 Å). However, for its C-12′ epimer **2**, although the indole diketopiperazine fragment showed similar interactions with the Top1-derived peptide binding pocket to that of **1**, the steroid moiety could not insert into the catalytic pocket due to the steric effect and faced the solvent region (Fig. 4). Interestingly, neither the steroid monomer ergosta-5,7,22-trien-3-ol nor the indole diketopiperazine alkaloid neoechinulin B showed significant Tdp1 inhibitory effect even at the concentration of 100 μmol/L, indicating

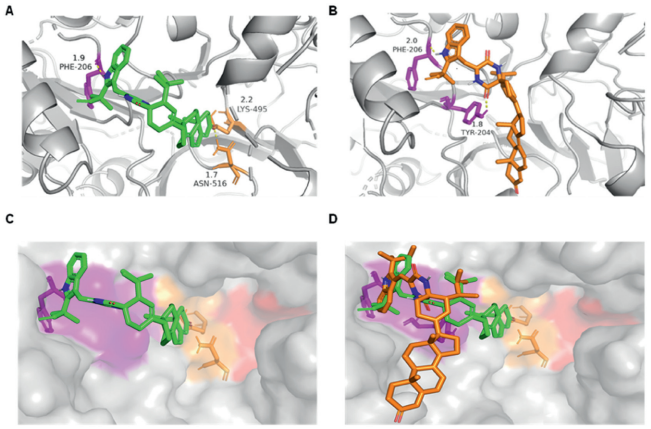


Fig. 4. Hypothetical binding mode of compounds **1** and **2** in the complex with Tdp1 (PDB: 6w4r). (A) Hypothetical binding mode of **1**. (B) Hypothetical binding mode of **2**. (C) Bound **1** with Tdp1 catalytic pocket colored orange, bound **1** with Top1-derived peptide-binding pocket colored purple, DNA-binding pocket colored red. (D) Superimposed poses of **1** (green) and **2** (orange) in the complex with Tdp1.

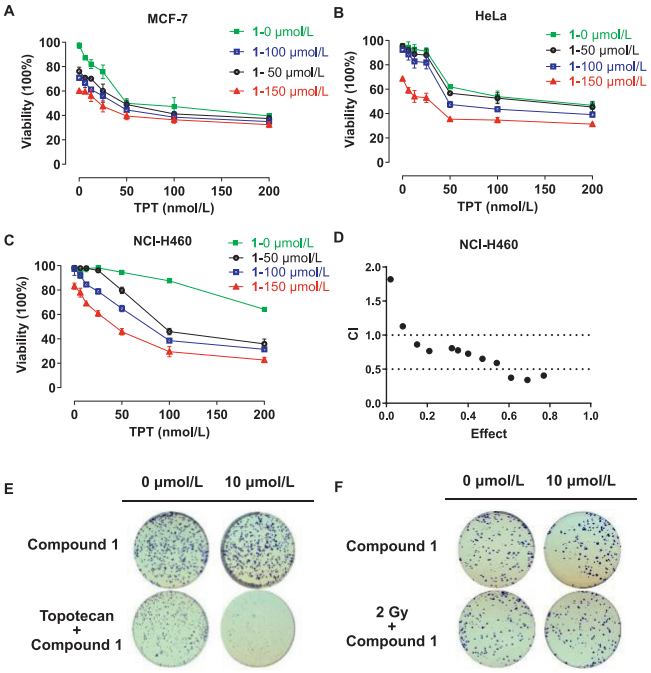


Fig. 5. Antitumor effects and sensitizing effects of **1**. Synergistic effect of **1** with topotecan in (A) MCF-7, (B) HeLa, and (C) NCI-H460 cells. (D) Combination index of **1** with topotecan in the NCI-H460 cells. (E) Clone formation of **1** with topotecan in the NCI-H460 cells. (F) Clone formation of **1** with radiation in the NCI-H460 cells. Data are presented as mean ± standard deviation (SD) ($n = 3$).

the fatal role of hybridization of these biosynthetic precursors and the synergistic regulation of Top1-derived peptide binding pocket and catalytic pocket. At present, almost all reported Tdp1 inhibitors are in a single binding mode with catalytic residues only [25], suggesting **1** could present as a new class of Tdp1 inhibitor.

To determine the role of Tdp1 inhibition by **1** in cancer cells, we examined its death effect in three cancer cell lines. As shown in Fig. 5, treatment of compound **1** alone did not induce significant cell death of MCF-7, HeLa, and NCI-H460 cells, but **1** showed selective synergistic antitumor effect against NCI-H460 cells while sparing the other two cancer cells when combined with topotecan. In addition, the sensitization assay showed that, **1** significantly increased the sensitivity of NCI-H460 cells to topotecan, even at the very low concentrations, while showed no sensitization effect

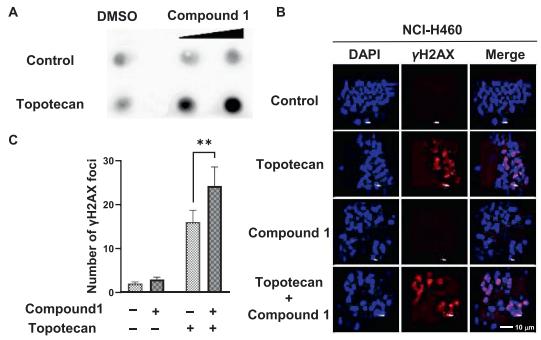


Fig. 6. (A) Stabilizing the formation of DNA–Tdp1 covalent cleavage complexes by *in vivo* complex of enzyme assay in H460 cells. (B) Histone γH2AX foci (red) induced by **1** alone and combine with topotecan in H460 cells. DAPI, 4′,6-diamidino-2-phenylindole. Scale bar: 10 μm. (C) Quantification of the number of γH2AX foci. Data are presented as mean ± SD ($n = 3$). $^{**}P < 0.01$.

under radiotherapy conditions (Fig. S6 in Supporting information). These evidences demonstrated compound **1**, with promising Tdp1 inhibitory effect, as a novel chemosensitizer when combined with chemotherapeutic Top1 inhibitors.

During the Tdp1-mediated DNA repairment, Tdp1 form transient Tdp1-DNA cleavage complexes (Tdp1cc) by releasing Top1 from Top1cc *via* hydrolyzing the 3′-phosphotyrosyl bonds [26]. Then, Tdp1cc are dissociated and releasing Tdp1, thus completing the DNA repair [27]. To investigate whether the chemosensitizing effect of **1** is related to its Tdp1 inhibitory effect, the immunocomplex of enzyme to DNA assay was performed. As shown in Fig. 6, **1** combined with topotecan stabilized the formation of cellular Tdp1cc in a dose-dependent manner. Meanwhile, **1** significantly upregulated the topotecan-induced γH2AX foci ($P < 0.01$), a classical DNA damage marker, in NCI-H460 cells.

Proteins are stereoscopic macromolecules with diverse chiral centers. From this perspective, natural products with complex stereochemical features may serve as instinctive ligands to certain proteins. In this paper, sterpiperazines A (**1**) and B (**2**), representing the first examples of steroid-based indole alkaloids were isolated from a soft coral-derived fungus as environmental-induced metabolites. Structurally, these marine natural products are identical in the highly stereoscopic steroidal tetracyclic scaffold and the planar aromatic indole fragment, but differ in the stereoisomeric configurations of the spirocyclic connection. Interestingly, in the biological studies, compound **1** notably enhanced the sensitivity of NCI-H460 cells to chemotherapy agents through inhibition of Tdp1 *via* a distinct binding mode, whereas its epimer **2** exhibited reduced potency. In summary, the discovery of **1** as unique environmental-induced metabolite highlights the significance of natural products in drug development [28], and provide a new chemical backbone for developing novel Tdp1 inhibitors.

Declaration of competing interest

The authors declare that they have no known competing financial interests or personal relationships that could have appeared to influence the work reported in this paper.

CRediT authorship contribution statement

Xia Wei: Writing – review & editing, Writing – original draft, Investigation, Data curation. **Zheng-Wu Luo:** Investigation. **Guo-Qiang Zhang:** Writing – original draft, Data curation. **Yan-An Lin:** Data curation. **Ze-Kun Zhang:** Investigation. **Lin-Kun An:** Methodology, Data curation. **Xi-Xin He:** Data curation. **Jun-Cheng Su:** Writing – review & editing, Supervision, Project administration. **Cui-Xian Zhang:** Writing – review & editing, Supervision, Funding acquisition, Conceptualization.

Acknowledgments

The work was financially supported by the National Natural Science Foundation of China (Nos. 82273845, 82304331, and 82360695) and Guangxi Natural Science Foundation project (No. 2023GXNSFBA026305). This paper is dedicated to Profs. Long-Mei Zeng and Jing-Yu Su (School of Chemistry and Chemical Engineering, Sun Yat-sen University) on the occasion of their 95th birthday.

Supplementary materials

Supplementary material associated with this article can be found, in the online version, at doi:10.1016/j.cclet.2025.111048.

References

[1] M. Macheret, T.D. Halazonetis, Annu. Rev. Pathol. 10 (2015) 425–448.
[2] H. Gaillard, T. Garcia-Muse, A. Aguilera, Nat. Rev. Cancer 15 (2015) 276–289.
[3] A. Rahman, P. O'Sullivan, I. Rozas, Med. Chem. Commun. 10 (2019) 26–40.
[4] A. Talukdar, B. Kundu, D. Sarkar, et al., Eur. J. Med. Chem. 236 (2022) 114304.
[5] C. Bailly, Pharmacol. Res. 148 (2019) 104398.
[6] L.R.H. Krumpe, B.A.P. Wilson, C. Marchand, et al., J. Am. Chem. Soc. 142 (2020) 21178–21188.
[7] Y. Pommier, A. Nussenzweig, S. Takeda, et al., Nat. Rev. Mol. Cell Biol. 23 (2022) 407–427.
[8] H.B. Wang, X.X. Bai, Y.H. Huang, et al., Chin. Chem. Lett. 34 (2023) 107671.
[9] X.W. Li, S.J. Fang, Y.Z. Li, et al., Bioorg. Chem. 143 (2024) 107015.
[10] R.X. Huang, P.K. Zhou, Signal Transduct. Target. Ther. 5 (2020) 60.
[11] R.X. Huang, P.K. Zhou, Signal Transduct. Target Ther. 6 (2021) 254.
[12] Q.Z. Dai, J.W. Chen, C.M. Gao, et al., Chin. Chem. Lett. 31 (2020) 404–408.
[13] F.J. Groelly, M. Fawkes, R.A. Dagg, et al., Nat. Rev. Cancer 23 (2023) 78–94.
[14] S. Watson, B. Verret, S. Ropert, et al., Cancer Med. 12 (2023) 3160–3166.
[15] S. Zhu, T. Zhang, L. Zheng, et al., J. Hematol. Oncol. 14 (2021) 156.
[16] F.A. Sofi, N. Tabassum, J. Biomol. Struct. Dyn. 41 (2023) 8605–8628.
[17] D.L. Chen, J.W. Li, X.D. Xu, et al., Chin. Chem. Lett. 35 (2024) 109451.
[18] D. Domingo-Fernández, Y. Gadiya, A.J. Preto, et al., J. Nat. Prod. 87 (2024) 1844–1851.
[19] H.R. Wu, C.N. Zhang, B.Q. Dou, et al., Bioorg. Chem. 152 (2024) 107716.
[20] X. Wei, J.C. Su, J.S. Hu, et al., Org. Lett. 24 (2022) 158–163.
[21] H. Zhang, Y. Xiong, D. Su, et al., Nat. Commun. 13 (2022) 4240.
[22] S.S. Laev, N.F. Salakhutdinov, O.I. Lavrik, Bioorgan. Med. Chem. 24 (2016) 5017–5027.
[23] K. Kovaleva, O. Yarovaya, K. Ponomarev, et al., Pharmaceuticals 14 (2021) 422.
[24] T.S. Dexheimer, L.K. Gediya, A.G. Stephen, et al., J. Med. Chem. 52 (2009) 7122–7131.
[25] X.Z. Zhao, E. Kiselev, G.T. Lountos, et al., Chem. Sci. 12 (2021) 3876–3884.
[26] L. Debéthune, G. Kohlhagen, A. Grandas, et al., Nucleic Acids Res. 30 (2002) 1198–1204.
[27] J.J. Pouliot, K.C. Yao, C.A. Robertson, et al., Science 286 (1999) 552–555.
[28] C. Li, Y.Y. Han, Y.N. Zhai, et al., Chin. Chem. Lett. 35 (2024) 109019.